THE PENNSYLVANIA STATE UNIVERSITY
SCHREYER HONORS COLLEGE

DEPARTMENT OF CHEMISTRY

MECHANISTIC AND SYNTHETIC APPROACHES TO NANOPARTICLE GROWTH AND ASSEMBLY

SARAH BEVILACQUA
SPRING 2017

A thesis
submitted in partial fulfillment
of the requirements
for a baccalaureate degree in Chemistry
with honors in Chemistry

Reviewed and approved* by the following:

Raymond Schaak
DuPont Professor of Materials Chemistry
Thesis Supervisor

Raymond Funk
Professor of Chemistry
Honors Adviser

Ben Lear
Associate Professor of Chemistry
Faculty Reader

* Signatures are on file in the Schreyer Honors College.

ABSTRACT

This study aims to understand the nitridation mechanism of Cu3PdN, which along with Cu3N, are the only transition metal nitrides that can be prepared colloidally under mild reaction conditions. Experiments were performed aiming to identify the source of nitrogen in nitride formation, as well as isolating other intermediates that might be present during the reaction. Preliminary results indicate that the use of nitrate salt and a primary amine is required for nitride formation. A spherical intermediate was also isolated; however, its identification was inconclusive. Lastly, attempt to intercalate palladium into preformed Cu3N did not lead to the formation of Cu3PdN. Further work is required to confirm the source of nitrogen and identify the reactive nitrogen species in this reaction.

Hybrid materials are important for their application as optoelectronic materials, electrochemical materials, and heterogeneous catalysts. However, methods for the spatially selective synthesis of these higher order nanoparticle assembly remains limited. A novel strategy to assemble nanoparticles is being developed using nanoparticles with spatially separated ligands. Functionalization of the ligands with furan or maleimide allows for particle coupling via the Diels Alder reaction. This report focuses on the synthesis of ligands for the coupling reaction, which will be tested in the coupling of gold nanosphere and nanorod. The process will allow for the assembly of new metal pairs that would not combine based on previously developed methods.

TABLE OF CONTENTS

LIST OF FIGURES

LIST OF TABLES

ACKNOWLEDGEMENTS

I would first like to thank Professor Ray Schaak for letting me do research in his lab for the past year and a half. He has mentored me in numerous ways and always made sure I was mentally challenged and reaching my full potential.

In addition, I would also like to thank my amazing mentor, Dr. Jamie Chen, for helping me in numerous ways every day. Her advice and insight were invaluable tools when conducting research and her vast knowledge of synthesis and catalysis taught me more than I could ever learn in a class. More than anything else, her remarkable patience when faced with my many mistakes and very rough drafts of proposals, applications, and thesis chapters was truly remarkable and always encouraged me to continue working. Thank you for always taking the time to help me further my education and mentoring me inside and outside of the lab.

Moreover, I would like to thank all members of the Schaak lab for their guidance, unending humor, and shared appreciation of Penn Kebab. I could turn to anyone in lab for help and found friends in all of you. Thank you for making every day memorable and recording all of my minor successes on our calendar.

I would lastly like to thank everyone else who made this thesis possible. Thank you to Professors Ray Funk and Ben Lear for taking the time to read and edit my thesis. My friends, roommates, and professors were a constant support system and always reminded me of the bigger picture and why I chose chemistry. Finally, I would like to thank my parents for all of their support and unconditional love. They fostered my love of chemistry and truly made me the nerd I am today. Thank you for challenging me to be a better person and reminding me to have fun along the way.

Chapter 1

Introduction to Thesis

Because colloidal syntheses occur at lower temperatures than corresponding solid state syntheses, one significant bottleneck in creating nanoparticles becomes finding reactants with a low energy barrier at solution temperatures. To investigate this problem, I looked at strategic model systems to understand mechanistic details of a synthesis. Another challenge in nanochemistry is the inability to effectively assemble nanoparticles with spatial selectivity, akin to the synthesis of a complex organic molecule from its synthons. I worked towards a novel assembly strategy which targets a wide range of materials to advance capabilities in colloidal nano-assembly.

Understanding Nanoparticle Formation

While the field of nanochemistry is rapidly growing and advancing, many fundamental questions regarding nanoparticle formation remain unanswered. Significant research has been done on the phase and morphologically controlled synthesis of nanocrystals to be used as semiconductors, heterogeneous catalysts, and photoactive materials, however, little is known regarding the mechanism and kinetics of colloidal reactions.[1,2,3]

One such example is a study of the mechanism and kinetics of formation of metal chalcogenide nanocrystals, which are commonly used as semiconductors and synthesized colloidally.[56] Kinetic experiments were performed using *in situ* NMR to probe the identity of the

chalcogenide precursors.[5] This mechanistic work was driven by a desire to improve shape control of the semiconductor nanocrystals, which is important in dictating the physical properties of the nanocrystal. By understanding the kinetics on the reaction pathways, scientists were able to scale up the nanocrystal syntheses and produce pure crystals (CdSe) on large scales in high yields.[5,7] Moreover, mechanistic understandings provided chemists with the ability to devise sequential reactions with better prediction of the end geometry and regiochemistry.[8] However, fully understanding intermediate steps and determining reaction mechanisms remain challenging in this field.

While formation mechanisms are beginning to be studied, mixed metal nitrides have garnered little attention despite having been frequently studied for their application as optoelectronic and electrochemical materials in addition to heterogeneous catalysts.[9–12] First-row transition metal nitride nanoparticles are rare as most of their syntheses require temperatures greater than 800 ^{o}C.[13–15] However, Cu_3PdN can be synthesized colloidally from $Cu(NO_3)_2 \cdot 3H_2O$, $Pd(acac)_2$, and a solvent mixture of oleylamine and 1-ocadecene at temperatures below 220 ^{o}C in less than an hour.[16] The relative ease of this reaction makes Cu_3PdN a model ternary metal nitride system to study. Understanding how nitrogen is incorporated in the final product would give insight into the reactive nitrogen species present and would aid in the development of syntheses of other mixed metal nitrides.

Motivated by the desire to better understand how ternary metal nitride nanoparticles form and to prepare new transition metal nitrides colloidally, my thesis investigates the source of nitrogen and identifies possible intermediates in the colloidal synthesis of Cu_3PdN.

Understanding Nanoparticle Assembly

Nanoparticle assembly into dimers, tetramers, and larger macrostructures can lead to improved or novel biomedical materials, optical sensors, and catalytic systems.[17]

Two common ways that nanoparticles assemble are through the application of external fields and through molecular interactions.[18] Nanoparticles can self-assemble upon the application of external magnetic, electric, and flow fields. When exposed to a magnetic or electric field, nanoparticles tend to polarize, creating an induced field and leading to dipole-dipole interactions between particles.[19] These fields are easy to apply and can work in combination with flow fields to produce better directed self-assembly. A flow field is any type of viscous movement applied to a medium; it can be oscillatory or steady and the organization is dependent on shear strain, shear rate, and particle volume fraction among other variables.[20] While these fields are effective at organizing nanoparticles, often the crystals go back to their disordered state once the field is removed. Therefore, if an equilibrium towards the ordered state is desired, scientists will tend to rely more on molecular interaction-based directed self-assembly.

Molecular interaction based self-assembly can be facilitated by temperature, light, pH, solvent polarity, or other reaction variables to change the interactions between nanoparticles. Many different morphologies such as flowers, spheres, chains, and bundles can be created simply by changing molecular interactions of the ligands on the nanoparticles.[18,21]

For example, the field of DNA controlled assembly of gold nanoparticles has expanded tremendously in the past two decades. Researchers can functionalize gold nanoparticles with DNA by taking advantage of the strong Au-S bond formed between cysteine and the particle. Through DNA's complimentary base-pair binding, the nanoparticles can form networks or discrete

assemblies with a high level of control[22,23]. However, these studies have been primarily confined to gold particles and, due to the use of DNA, can only be done under aqueous conditions.[21,22,24]

To overcome these limitations, I have been focusing on developing robust organic ligands that will eventually be amenable to the assembly nanoparticle materials beyond gold and in non-aqueous conditions. Furthermore, by functionalizing the non-particle binding end of the ligands with furan or maleimide, these moieties undergo the forward Diels Alder reaction easily at 60 °C and the reaction is reversible at 90°C, allowing for reversible particle assembly. Through attempts to expand directed self-assembly to new classes of nanoparticles, my thesis works towards one of the ultimate goals of nanochemistry: using nanoparticles as "artificial atoms" upon which higher order hybrid nanostructures can be built.

References

1. Davis, R. F. III-V nitrides for electronic and optoelectronic applications. *Proc. IEEE* **79,** 702–712 (1991).
2. Moriya, Y., Takata, T. & Domen, K. Recent progress in the development of (oxy)nitride photocatalysts for water splitting under visible-light irradiation. *Coord. Chem. Rev.* **257,** 1957–1969 (2013).
3. Orton, J. W. & Foxon, C. T. Group III nitride semiconductors for short wavelength light-emitting devices. *Reports Prog. Phys.* **61,** 1–75 (1998).
4. Meen, T.-H. *et al.* Surface plasma resonant effect of gold nanoparticles on the photoelectrodes of dye-sensitized solar cells. *Nanoscale Res. Lett.* **8,** 450 (2013).
5. García-Rodríguez, R., Hendricks, M. P., Cossairt, B. M., Liu, H. & Owen, J. S. Conversion Reactions of Cadmium Chalcogenide Nanocrystal Precursors. doi:10.1021/cm3035642
6. Peng, X. Mechanisms for the Shape-Control and Shape-Evolution of Colloidal Semiconductor Nanocrystals. *Adv. Mater.* **15,** 459–463 (2003).
7. Zhengtao Deng, Li Cao, Fangqiong Tang, & Bingsuo Zou. A New Route to Zinc-Blende CdSe Nanocrystals: Mechanism and Synthesis. (2005). doi:10.1021/JP052484X
8. Schaak, R. E. & Williams, M. E. Full Disclosure: The Practical Side of Nanoscale Total Synthesis. *ACS Nano* **6,** 8492–8497 (2012).
9. Wu, H. & Chen, W. Copper Nitride Nanocubes: Size-Controlled Synthesis and Application as Cathode Catalyst in Alkaline Fuel Cells. *J. Am. Chem. Soc.* **133,** 15236–

15239 (2011).
10. Zerr, A. *et al.* Recent Advances in New Hard High-Pressure Nitrides. *Adv. Mater.* **18,** 2933–2948 (2006).
11. Lee, B. S. *et al.* Copper nitride nanoparticles supported on a superparamagnetic mesoporous microsphere for toxic-free click chemistryw. doi:10.1039/c001255f
12. Hargreaves, J. S. J. Heterogeneous catalysis with metal nitrides. *Coord. Chem. Rev.* **257,** 2015–2031 (2013).
13. Nagai, M. Transition-metal nitrides for hydrotreating catalyst—Synthesis, surface properties, and reactivities. *Appl. Catal. A Gen.* **322,** 178–190 (2007).
14. Young, A. F. *et al.* Synthesis of Novel Transition Metal Nitrides IrN_2 and OsN_2. *Phys. Rev. Lett.* **96,** 155501 (2006).
15. Hasegawa, M. & Yagi, T. Systematic study of formation and crystal structure of 3d-transition metal nitrides synthesized in a supercritical nitrogen fluid under 10 GPa and 1800K using diamond anvil cell and YAG laser heating. *J. Alloys Compd.* **403,** 131–142 (2005).
16. Vaughn II, D. D. *et al.* Solution Synthesis of Cu_3PdN Nanocrystals as Ternary Metal Nitride Electrocatalysts for the Oxygen Reduction Reaction. *Chem. Mater.* **26,** 6226–6232 (2014).
17. Busseron, E., Ruff, Y., Moulin, E. & Giuseppone, N. Supramolecular self-assemblies as functional nanomaterials. *Nanoscale* **5,** 7098 (2013).
18. Grzelczak, M., Vermant, J., Furst, E. M. & Liz-Marzá, L. M. Directed Self-Assembly of Nanoparticles. doi:10.1021/nn100869j
19. Gast, A. P. & Zukoski, C. F. Electrorheological fluids as colloidal suspensions. *Adv. Colloid Interface Sci.* **30,** 153–202 (1989).
20. Stancik, E. J. *et al.* Structure and dynamics of particle monolayers at a liquid–liquid interface subjected to shear flow. *Faraday Discuss.* **123,** 145–156 (2003).
21. Westerlund, F. & Bjørnholm, T. Directed assembly of gold nanoparticles. *Curr. Opin. Colloid Interface Sci.* **14,** 126–134 (2009).
22. Mirkin, C. A., Letsinger, R. L., Mucic, R. C. & Storhoff, J. J. A DNA-based method for rationally assembling nanoparticles into macroscopic materials. *Nature* **382,** 607–609 (1996).
23. Alivisatos, A. P. *et al.* Organization of 'nanocrystal molecules' using DNA. *Nature* **382,** 609–611 (1996).
24. Ho, M. L. *et al.* 15-Crown-5 functionalized au nanoparticles synthesized via single molecule exchange on silica nanoparticles: its application to probe 15-crown-5/k +/15-crown-5 'sandwiches' aslinking mechanisms. © 2009 American Chemical Society. *J. Phys. Chem. C* **113,** 1686–1693 (2009).

Chapter 2

Mechanistic study of metal nitrides

Introduction

Due to the small size of nanoparticles, the field of nanochemistry presents materials with unusual structural and optical properties. The particles, typically on the order of 1-100 nm, exhibit quantum effects, making them interesting photoactive and electrooptical materials. Furthermore, the high surface area to volume ratio and the ability to control shape, size, and composition, make nanoparticles successful heterogeneous catalysts. Due to these applications, much of nanochemistry is function driven.

One promising group of nanoparticles with interesting opto- and electro-properties are transition metal nitrides. This class of materials are commonly used as optoelectronic devices and heterogeneous catalysts due to their high surface area and ability to release nitrogen from the bulk lattice, creating new active sites *in situ.*[1] Most transition metal nitrides are synthesized between 700-1200 K but there are syntheses reporting reaction conditions as high as 2000 K.[1–3] These temperatures are not amenable to colloidal synthesis and therefore limiting the application of transition metal nitride nanoparticles.

I studied two copper nitrides, Cu_3N and Cu_3PdN, due to their relative ease of formation compared to other transition metal nitrides.[1,4] The following experiments were done in collaboration with Dr. Jamie Chen and Catherine Badding.

Cu_3N can be colloidally synthesized with a copper nitrate salt, $Cu(NO_3)_2 \cdot 3H_2O$, in addition to oleylamine and 1-octadecene. To synthesize Cu_3N, the reaction needs to be heated to at least 190 °C for at least an hour.

Interestingly, Cu_3PdN can be easily synthesized at lower temperatures. Nanoparticles can be colloidally synthesized from $Cu(NO_3)_2 \cdot 6H_2O$, $Pd(acac)_2$, and a solvent mixture of oleylamine and 1-ocadecene at 160 °C for 30 minutes.[5] The ability to use milder reaction conditions is striking and leads to the question of why Cu_3PdN forms easier than Cu_3N.

Previous work on Cu_3PdN focused on its catalytic ability. The antiperovskite nanocrystals are catalytically active (figure 1, left), reducing oxygen under alkaline conditions and oxidizing formic acid better than Cu_3N and Pd nanocrystals when controlled for mass activity.[5,6] The desire to improve these catalysts along with the possibility of colloidally synthesizing other transition metal nitrides motivated my mechanistic study of Cu_3PdN synthesis.

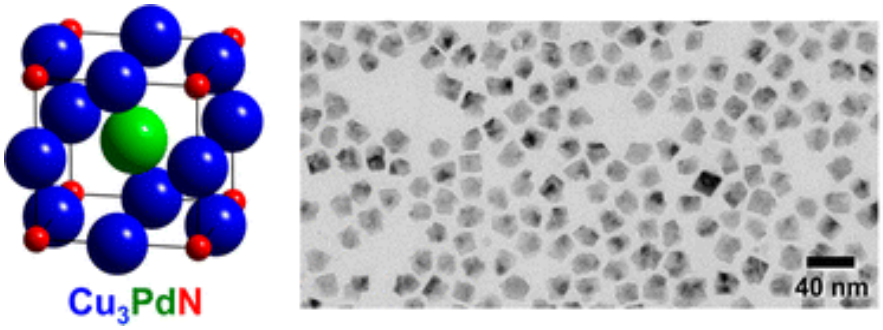

Figure 1. *Unit cell and TEM of Cu_3PdN nanoparticles.*

The first interesting aspect of the aforementioned synthesis is that Cu_3PdN can be prepared under such mild conditions. The temperature is relatively low and the reaction does not need to be done under a high pressure of N_2 or NH_3 atmosphere. Within the reaction, there are two nitrogen sources: the nitrate anion of the metal salt and the primary amine moiety in oleylamine, which serves as both a ligand and reductant. One study on Cu_3N used gas chromatography-mass

spectrometry to analyze organic byproducts throughout the reaction. The data suggested that ammonia generated in situ from benzylamine nitridated Cu(I) to form Cu_3N.[7] Being able to identify the source of nitrogen in the nitridation mechanism of Cu_3PdN would allow for synthetic extrapolation into other systems, possibly creating low energy reaction pathways to new transition metal nitride nanoparticles.[7]

Lastly, I attempted to determine the mechanism through which palladium is incorporated into the crystal structure presented in figure 1. Pd can first alloy with Cu, followed by nitridation, or Cu_3N could for first, followed by intercalation of Pd. Experiments were conducted to test these hypotheses.

Materials and Methods

Cu_3N: $Cu(NO_3)_2 \cdot 6\ H_2O$ (0.124 mmol), 1-octadecene (3.75 mL), and oleylamine (1.25mL) were dried at 120 °C under vacuum for 10 minutes. The solution was then mixed at 240 °C under argon for 60 minutes. After cooling the particles to room temperature, 12.5 mL of ethanol was added and the mixture was centrifuged at 12000 rpm for 5 minutes. The particles were washed three times with 1:1 toluene-ethanol and were suspended in hexanes.

Cu_3PdN: $Cu(NO_3)_2 \cdot 6\ H_2O$ (0.124 mmol), $Pd(acac)_2$ (0.0414 mmol), 1-octadecene (3.75 mL), and oleylamine (1.25 mL) were dried at 120 °C under vacuum for 10 minutes. The solution was then mixed at 150 °C under argon for 30 minutes. After cooling the particles to room temperature, 12.5 mL of ethanol was added and the mixture was centrifuged at 12000 rpm for 5 minutes. The particles were washed three times with 1:1 toluene-ethanol and were suspended in hexanes.

All other experiments were done under identical reaction conditions as listed above with changes noted in tables 1 and 2.

Results and Discussions

To determine the source of nitrogen of the metal nitrides, therefore learning more about the reactive nitrogen species present in this reaction, a series of control experiments were performed to determine the necessity of the nitrate anion. Following table 1, $Cu(NO_3)_2 \cdot 6\ H_2O$ was replaced with a non-nitrogenous copper salts to see if oleylamine was a suitable nitrogen donor on its own. Only Cu^{2+} salts were tested.

Table 1. *Control reactions for the necessity of nitrate anion in the synthesis of Cu_3N and Cu_3PdN*

Cu	Pd	Temp	Time	Product
$Cu(Cl)_2$	---	200 °C	3 hr	Amorphous
$Cu(OAc)_2$	---	200 °C	3 hr	Little precipitate, Cu
$Cu(acac)_2$	$Pd(acac)_2$	160 °C	1 hr	Cu_3Pd

While a Cu_3Pd alloy was formed by the acac salts, no reaction successfully produced Cu_3N or Cu_3PdN nanocrystals, showing that the nitrate salt was required for both reactions. Next, oleylamine was replaced with a variety of solvent to probe its necessity. Table 2 shows the reaction conditions tested (note that octadecene was used as a co-solvent in all reactions).

Table 2. *Control reactions for the necessity of oleylamine in the synthesis of Cu_3N and Cu_3PdN*

Cu	Pd	Other	Temp	Time	Product
$Cu(NO_3)_2$	$Pd(acac)_2$	Oleylamine	160 °C	1 hr	Cu_3PdN
$Cu(NO_3)_2$	$Pd(acac)_2$	Hexadecylamine	160 °C	1 hr	Cu_3PdN
$Cu(NO_3)_2$	$Pd(acac)_2$	Oleyl alcohol	160 °C	1 hr	Amorphous
$Cu(NO_3)_2$	$Pd(acac)_2$	Trioctylamine	160 °C	1 hr	Cu_3Pd
$Cu(NO_3)_2$	$Pd(acac)_2$	Trioctylphosphine	160 °C	1 hr	Cu_3Pd
$Cu(NO_3)_2$	$Pd(acac)_2$	Hexadecanediol	160 °C	1 hr	mixture
$Cu(NO_3)_2$	$Pd(acac)_2$	Morpholine borane, Oleic acid	160 °C	1 hr	Amorphous
$Cu(NO_3)_2$	$Pd(acac)_2$	Oleic acid	160 °C	1 hr	CuPd

The first experiment was done by exchanging oleylamine with hexadecylamine. Hexadecylamine maintains the primary amine functionality present in oleylamine but without a double bond moiety at C9. This reaction went forward as predicted, showing that an alkene was unnecessary for nitride formation. Next, oleyl alcohol, the alcohol analogue of oleylamine, was tested and did not produce any product, showing the necessity of an amine. Trioctylamine, a tertiary amine solvent, produced only the Cu_3Pd alloy, which demonstrated the need for a primary amine in the reaction. To try other solvents with similar polarity, hexadecanediol and oleic acid were tested, but neither produced the desired product. Morpholine borane was introduced as an added reducing agent when no reductant was present in the reaction. Overall, a primary amine was

needed for successful synthesis of Cu_3PdN. The XRD patterns for the experiments are shown below.

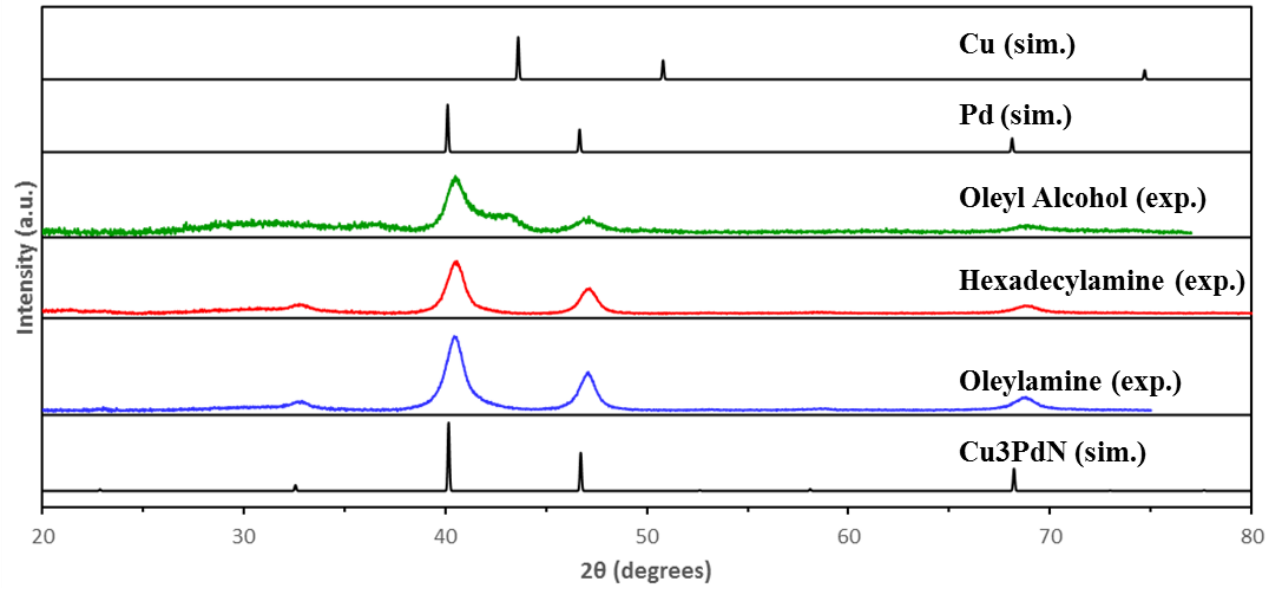

Figure 2. *XRD corresponding to Table 2 entries 1 (blue), 2 (red), 3 (green).*

The XRD shows that both oleylamine and hexadecylamine produced Cu_3PdN. The oleyl alcohol reaction produced peaks that could correspond to Pd or Cu_3PdN. However, it is difficult to observe the distinguishing peak at 33°, thus giving inconclusive results. There is evidence of a copper peak, but again is hard to draw conclusive results.

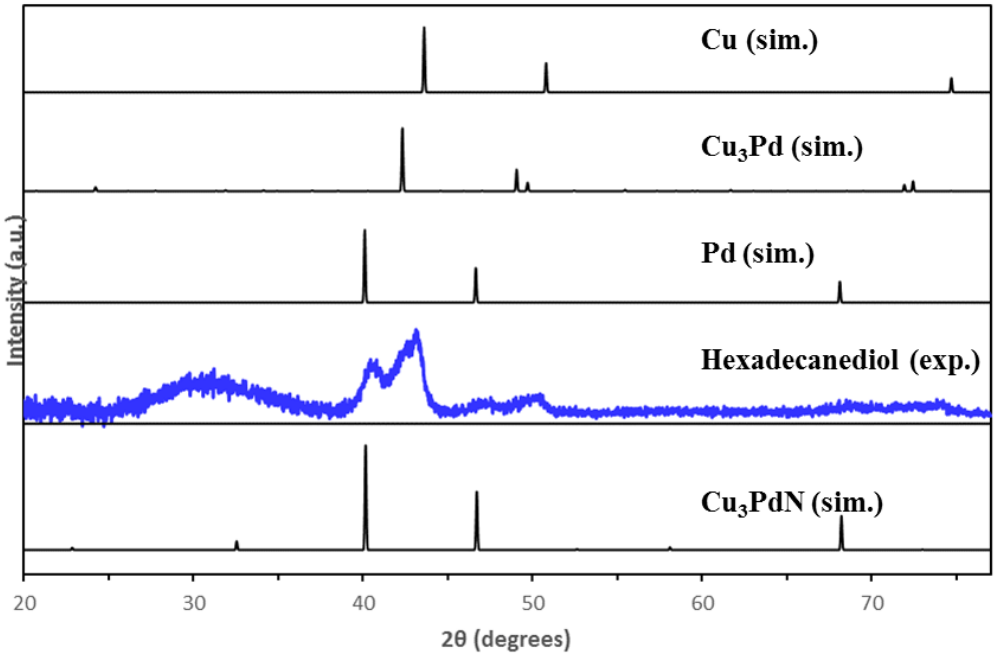

Figure 3. *XRD corresponding to Table 2 entry 6 (blue).*

When using a different alcohol solvent, hexadecanediol, we only see a mixture of metals. While still giving a broad XRD pattern, there appears to be a set of peaks that lines up well with the reference XRD pattern of Pd, Cu, and Cu_3Pd, suggesting that the use of hexadecanediol produces a mixture of metals and alloys.

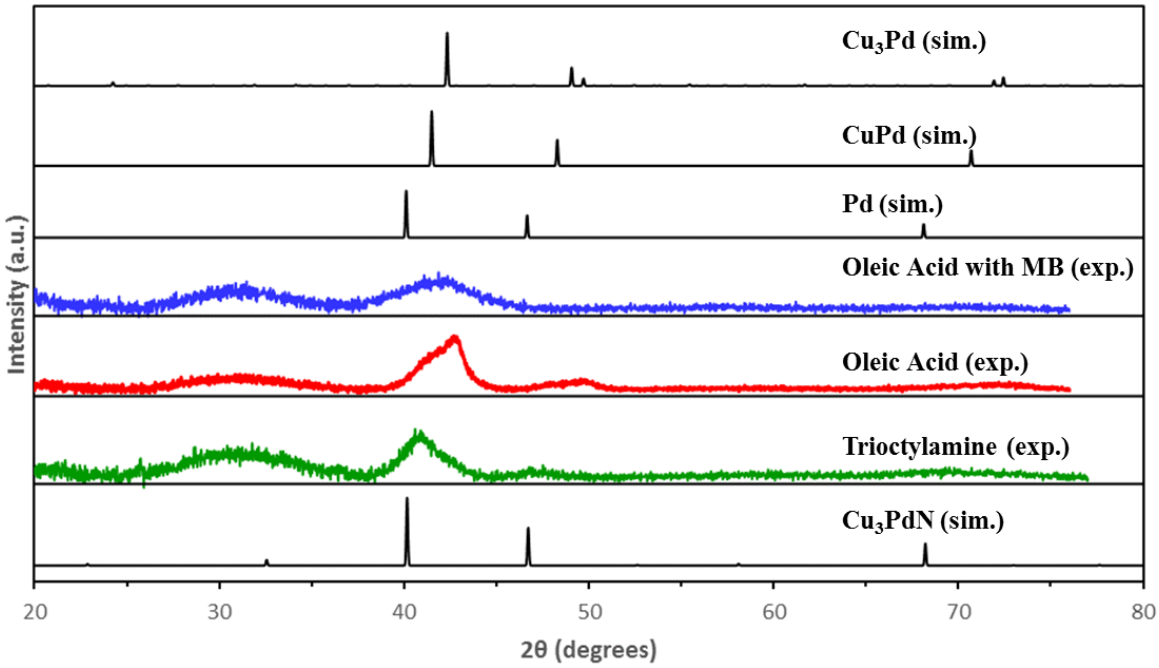

Figure 4. *XRD corresponding to Table 2 entries 4 (green), 8 (red), and 7 (blue).*

Looking at trioctylamine as a solvent, we only saw peaks matching to Pd, showing that a tertiary amine does not work. When using oleic acid with and without morpholine borane, we do not see the proper broad XRD patterns were observed. These experiments all suggest that a primary amine solvent is necessary for the proper synthesis for Cu_3PdN and Cu_3N. These control experiments showed that the nitridation of Cu_3PdN and Cu_3N does not occur simply through the decomposition of a nitrate salt or through oleylamine. Both reactants are needed and the mechanism at play involves a complex relationship between the two nitrogen sources. More experiments, such as nitrogen labeling and analysis of solution species, are required to better understand the nitridation mechanism.

A temperature study was performed to study intermediates in the synthesis of Cu_3PdN. First, Cu_3PdN was synthesized as reported in the Materials and Methods. Aliquots were taken at 150 °C, 180 °C, and 210 °C. The aliquots were analyzed by TEM and XRD.

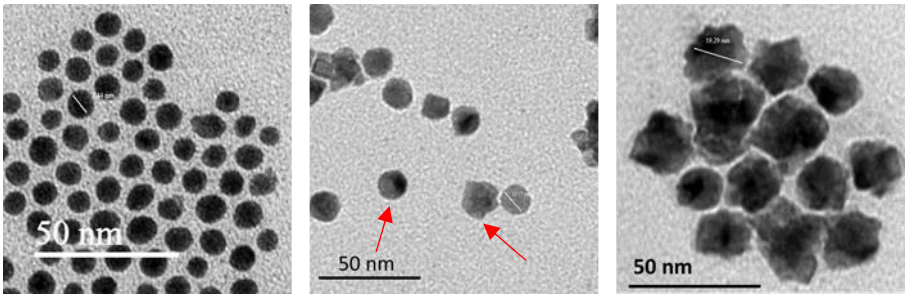

Figure 5. *TEM of Cu_3PdN at (left) 150 °C, (middle) 180 °C, and (right) 210 °C. Arrows in the TEM image of 180 °C reaction indicate the presence of both spherical and cubic particles*

At 150 °C, nanospheres were observed. This intermediate then starts becoming cubic at 180 °C. The TEM image in the middle shows both sphere and cubic structures, indicating that 180 °C is an important temperature within the synthesis. While I did not have time to further investigate the morphological change occurring at 180 °C, future studies could be done to determine how this change occurred. By 210 °C, TEM shows fully formed cubic particles.

To better characterize the spherical intermediate at 150 °C, aliquots were taken at 15 mins, 50 mins, and 210 mins while holding the temperature constant. Aliquots were also taken at 15 mins and 30 mins while holding the temperature at 160 °C.

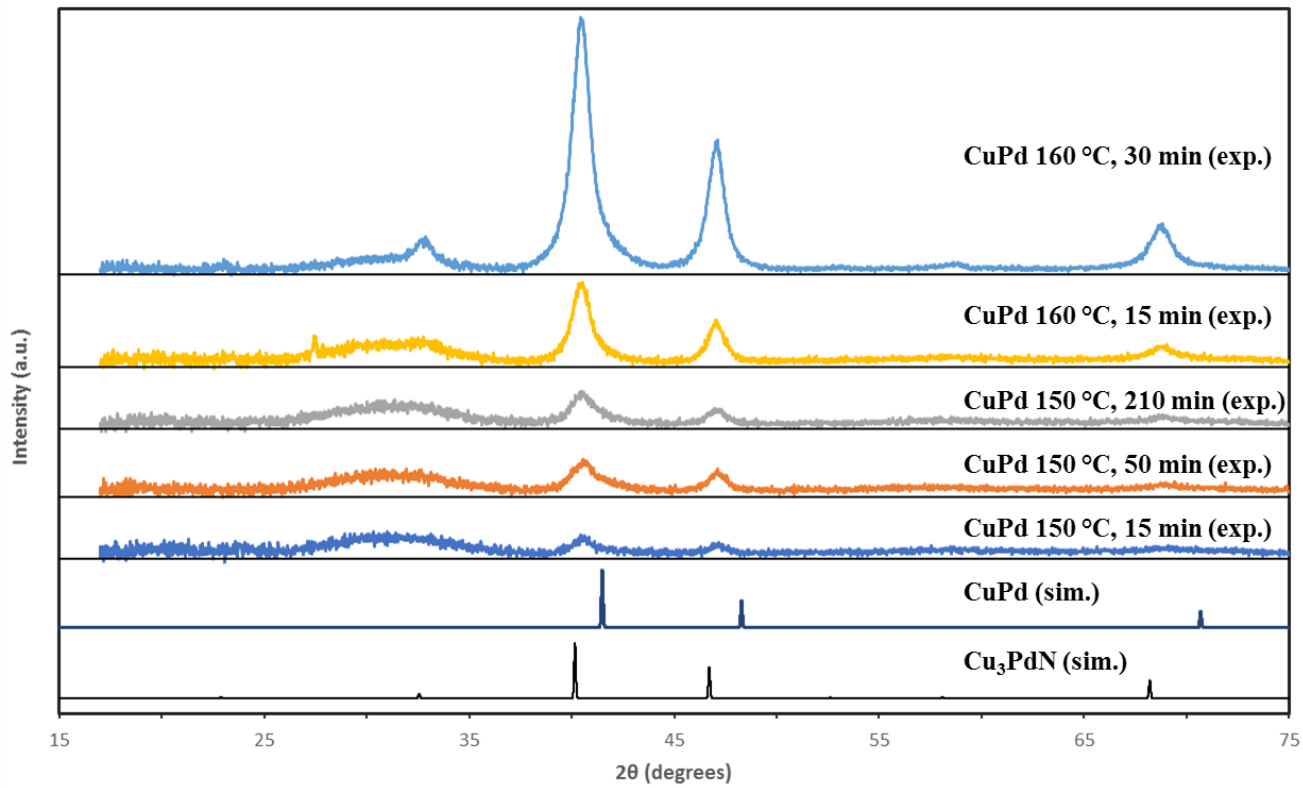

Figure 6. *XRD of CuPd alloy intermediate at 150 °C 15 min (dark blue); 150 °C 50 min (orange); 150 °C 210 min (gray); 160 °C 15 min (yellow); 160 °C 30 min (light blue).*

While XRD does confirm the eventual presence of Cu_3PdN at 160 °C, it is hard to rule out the possible presence of Cu_3PdN at 150 °C due to the broad amorphous peak at 30° coincides with the distinguishing small nitride peak at 32.5°. The patterns collected at 150 °C could signify the presence of Cu_3PdN with low crystallinity, however it also coincides well with the pattern of a palladium rich CuPd alloy. Therefore, it is possible that spherical Cu_3PdN nanoparticles are first formed and then morph into the cubic morphology. Because the traces at 150 °C signify the possibility of a CuPd alloy intermediate, we decided to separately synthesize CuPd and test if it is a viable starting material.

CuPd alloy was prepared separately and allowed to react with two equivalents of $Cu(NO_3)_2$. It was hypothesized that if CuPd is truly an intermediate, it should be able to react with the

remaining two equivalents of $Cu(NO_3)_2$ and produce Cu_3PdN. The reaction using CuPd alloy made from acac salts and oleylamine (as the reducing agent) did not lead to the formation of Cu_3PdN. However, when CuPd alloy particles were made using morpholine borane as the reductant (oleylamine still present), the formation of cubic Cu_3PdN was observed as shown in the XRD pattern and TEM image below (Figure 7).

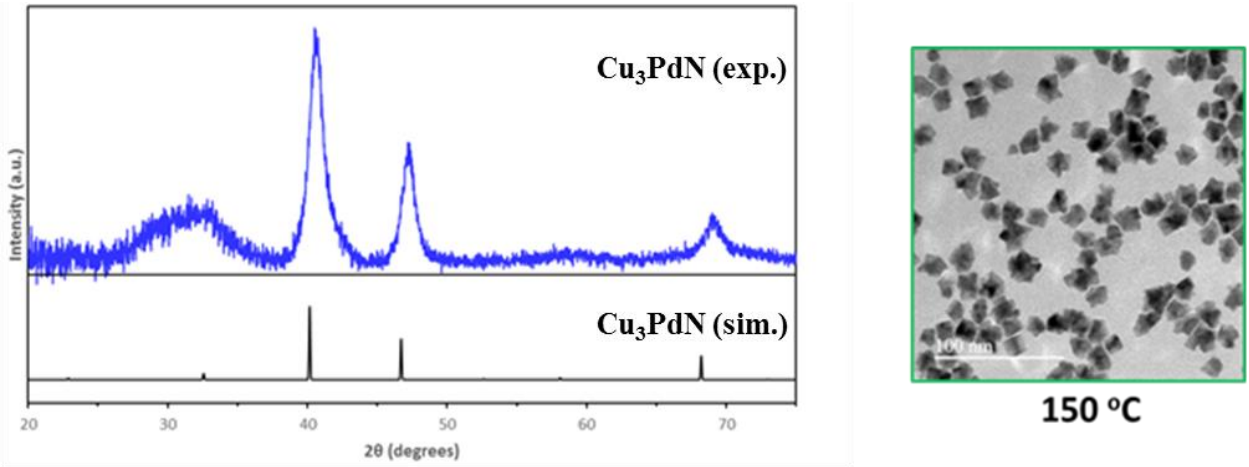

Figure 7. *XRD and TEM of Cu_3PdN from CuPd alloy and morpholine borane*

While a broad amorphous peak is observed in the XRD pattern, the small distinguishing nitride peak at 32.5° does seem to present. Combined with the observation of cubic particles, our results does indicate the successful synthesis of Cu_3PdN. The TEM below gives some insight into why morpholine borane produces an “active” CuPd alloy (Figure 8).

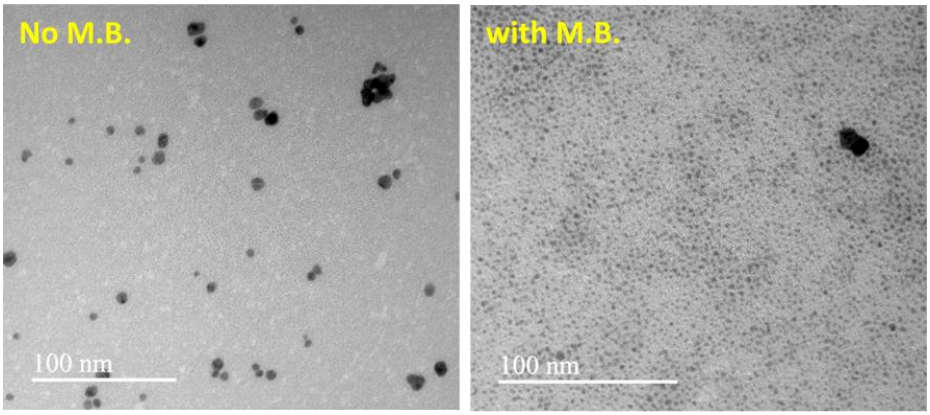

Figure 8. *TEM of CuPd alloy without (left) and with (right) morpholine borane.*

The CuPd alloy particles produced with morpholine borane are much smaller than those produced without it and the CuPd particles produced using just oleylamine resembled more of those that were isolated from the reaction of Cu_3PdN. It is possible that the small CuPd particles synthesized using morpholine borane could dissolve in solution, thus releasing soluble Pd species that can react with the copper nitrate in solution to produce cubic Cu_3PdN. The results of these experiments would suggest that it is more likely that CuPd alloy was not the intermediate isolated from the Cu_3PdN reaction, and that the initial product of the reaction is spherical Cu_3PdN.

Another possible mechanism for the formation of Cu_3PdN could be the intercalation of Pd into previously formed Cu_3N. To test this hypothesis, Cu_3N was first synthesized and then exposed to palladium salt. First, $Pd(acac)_2$ was mixed with three equivalents of Cu_3N under reducing condition to see if some Pd(0) species could intercalate into the lattice of the previously formed cubic anti-ReO_3 Cu_3N crystals. The reaction was heated up to 240 °C and aliquots were taken at various temperatures (Figure 9).

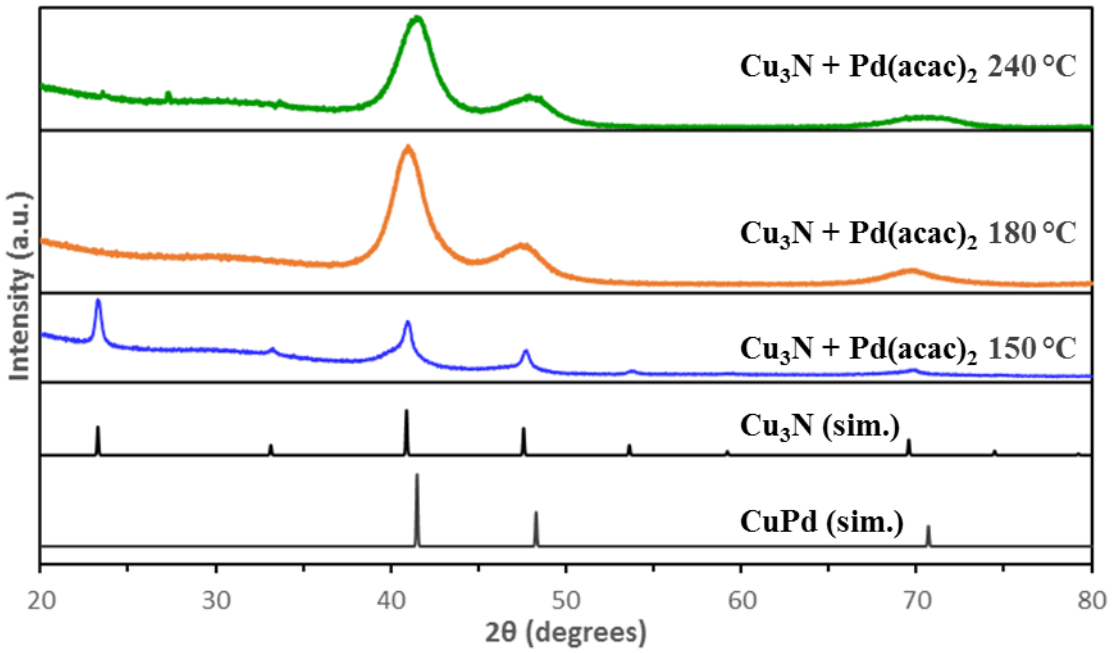

Figure 9. *XRD of Cu_3N and $Pd(acac)_2$ at 150 °C (blue) 180 °C (orange) and 240 °C (green).*

XRD shows the presence of Cu_3N at 150 °C. Even at low temperature, broadening of the peaks was observed, suggesting the presence of a second material. Once the mixture was heated to higher temperatures, crystalline Cu_3N pattern was lost and the pattern resembled amorphous CuPd. To further investigate the reaction, TEM images were taken of samples from each aliquot.

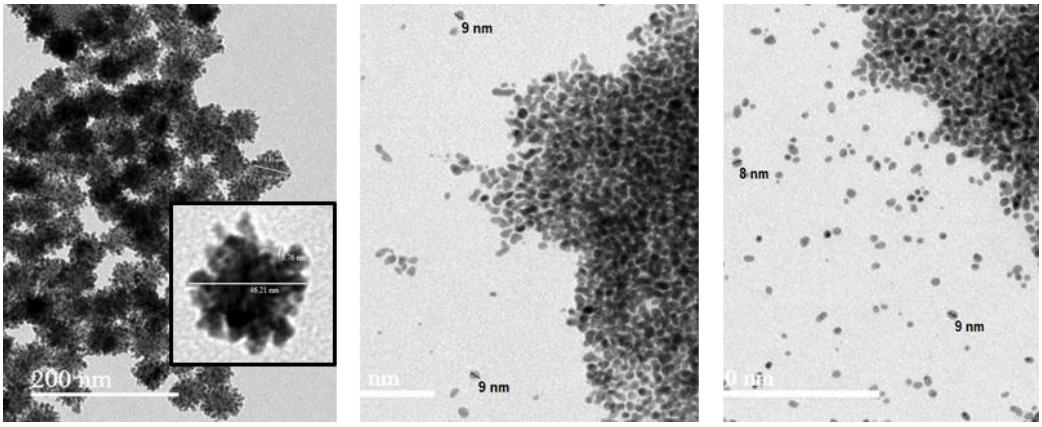

Figure 10. *TEM of Cu_3N and $Pd(acac)_2$ at 150 °C (left), 180 °C (middle), and 240 °C (right).*

The TEM image at 150 °C shows the expected Cu_3N cubes present at the beginning of the reaction. However, there appears to be Pd nanoparticles attaching to the outside the Cu_3N cubes. As the temperature increased, loss of the cubic particle was observed with the appearance of small irregularly shaped particles. XRD pattern indicated that these irregular particles are CuPd alloy (Figure 10) and Cu_3N is no longer present.

In conclusion, I saw that the nitridation of Cu_3N and Cu_3PdN involves a complex mechanism between the decomposition of oleylamine and the nitrate. Both reactants are required for the formation of pure crystalline material and a primary amine must also be present. To further study nitrogen incorporation, ^{15}N labeled $Cu(NO_3)_2$ will be used in the synthesis of Cu_3PdN and a decomposition study will be performed to determine the isotopic distribution of evolved N_2 gas. While preliminary TEM data showed evidence of a spherical intermediate in the synthesis of Cu_3PdN, the XRD trace inconclusively shows the presence of either CuPd or spherical Cu_3PdN. Lastly, we provided evidence that palladium does not intercalate into previously formed Cu_3N in the formation of Cu_3PdN.

References

1. Nagai, M. Transition-metal nitrides for hydrotreating catalyst—Synthesis, surface properties, and reactivities. *Appl. Catal. A Gen.* **322,** 178–190 (2007).
2. Young, A. F. *et al.* Synthesis of Novel Transition Metal Nitrides IrN_2 and OsN_2. *Phys. Rev. Lett.* **96,** 155501 (2006).
3. Hasegawa, M. & Yagi, T. Systematic study of formation and crystal structure of 3d-transition metal nitrides synthesized in a supercritical nitrogen fluid under 10 GPa and 1800K using diamond anvil cell and YAG laser heating. *J. Alloys Compd.* **403,** 131–142 (2005).
4. Zerr, A. *et al.* Recent Advances in New Hard High-Pressure Nitrides. *Adv. Mater.* **18,** 2933–2948 (2006).

5. Vaughn II, D. D. *et al.* Solution Synthesis of Cu_3PdN Nanocrystals as Ternary Metal Nitride Electrocatalysts for the Oxygen Reduction Reaction. *Chem. Mater.* **26,** 6226–6232 (2014).
6. Jia, J., Shao, M., Wang, G., Deng, W. & Wen, Z. *Cu_3PdN nanocrystals electrocatalyst for formic acid oxidation*. *Electrochemistry Communications* **71,** (2016).
7. Deshmukh, R. *et al.* Ultrasmall Cu_3N Nanoparticles: Surfactant-Free Solution-Phase Synthesis, Nitridation Mechanism, and Application for Lithium Storage. *Chem. Mater.* **27,** 8282–8288 (2015).

Chapter 3

Reversible self-assembly of colloidal nanoparticles

Introduction

The importance of organic molecules, ranging from pharmaceuticals to polymers to sensors, has made the development of selective methods for generating their complex molecular structures a thriving field of research for more than a century. In recent years, advances in nanoparticle synthesis have complemented organic chemistry advances tremendously, generating methods that allow for shape and phase control, leading to novel materials with a wide range of applications, from drug delivery and catalysis to energy storage and fuel cell.[1–3] However, despite these recent advances, the ability to selectively synthesize higher order nanostructures, analogous to the synthesis of large and complex molecules in organic chemistry, remains a formidable challenge. Being able to construct complex nanostructures from the selective assembly of individual nanoparticles allows for the incorporation of multifunctionality, such as a Z-scheme water splitting photo catalyst assembly.[4]

Unlike organic chemistry, only limited systems exist for building higher order nanostructures selectively. Our lab has demonstrated the synthesis of a Ag-Pt-Fe_3O_4 three-component hybrid nanoparticle and examined its formation pathway.

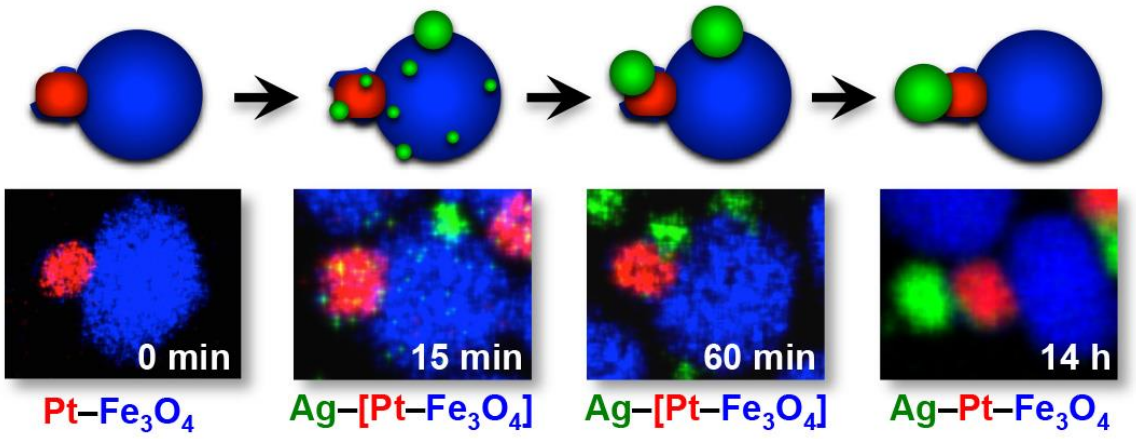

Figure 11. *Growth mechanism for the chemoselective synthesis of Ag-Pt-Fe3O4.*
Reproduced with permission from ref 5. Copyright 2015American Chemical Society

In this synthesis, Ag – Pt – Fe_3O_4 can be selectively grown over all other possible configuration of the three components. However, this prep relies strongly on the intrinsic thermodynamic properties of each metal and is not easily adaptable to other systems.[5] Therefore, the spatially selective assembly of any nanoparticle material remains a challenge that needs to be addressed.

A lot of work has been done on assembling Au nanoparticles as they can be functionalized with elaborately designed macroligands or polymers which is central to generating novel single unit multifunctional materials.[6,7] The Mirkin group has shown that DNA oligo-nucleotides bind tightly to gold nanoparticles through a thiol functional group, taking advantage of the strong S-Au bond. These particles can then be controllably assembled by placing complimentary DNA strands on different nanoparticles. The process can be reversed by thermal denaturation.[7] While nanoparticle assembly has made strides towards finely tuned reactions, synthesis and assembly of anisotropic particles via this method still needs to be developed.

Using a physical blocker is one method of generating anisotropic particles, and this method has been applied to a gold silica heteronanoparticle system.

Figure 12. *Anisotropic silica gold nanoparticles via physical blocking.*
Reproduced with permission from ref 8. Copyright 2014 Elsevier

As shown in figure 12, first gold nanoparticles are synthesized. Using the strong Au-S bond, the particles can be immobilized on thiol-terminated thin films deposited onto a glass sheet. Then, silica is grown onto the exposed surfaces of the gold particles but not on the side that has been blocked. The resulting asymmetric hemispherical silica gold nanoparticles are released via ultrasonication[8]. While these particles are anisotropic, they cannot easily undergo multiple ligand functionalization sequences as the silica shell would have to be removed under harsh conditions (HF or concentrated hydroxide solutions) to make use of the gold underneath.

One lab successfully spatially functionalized nanoparticles by taking advantage of hydrophobic and hydrophilic ligands.

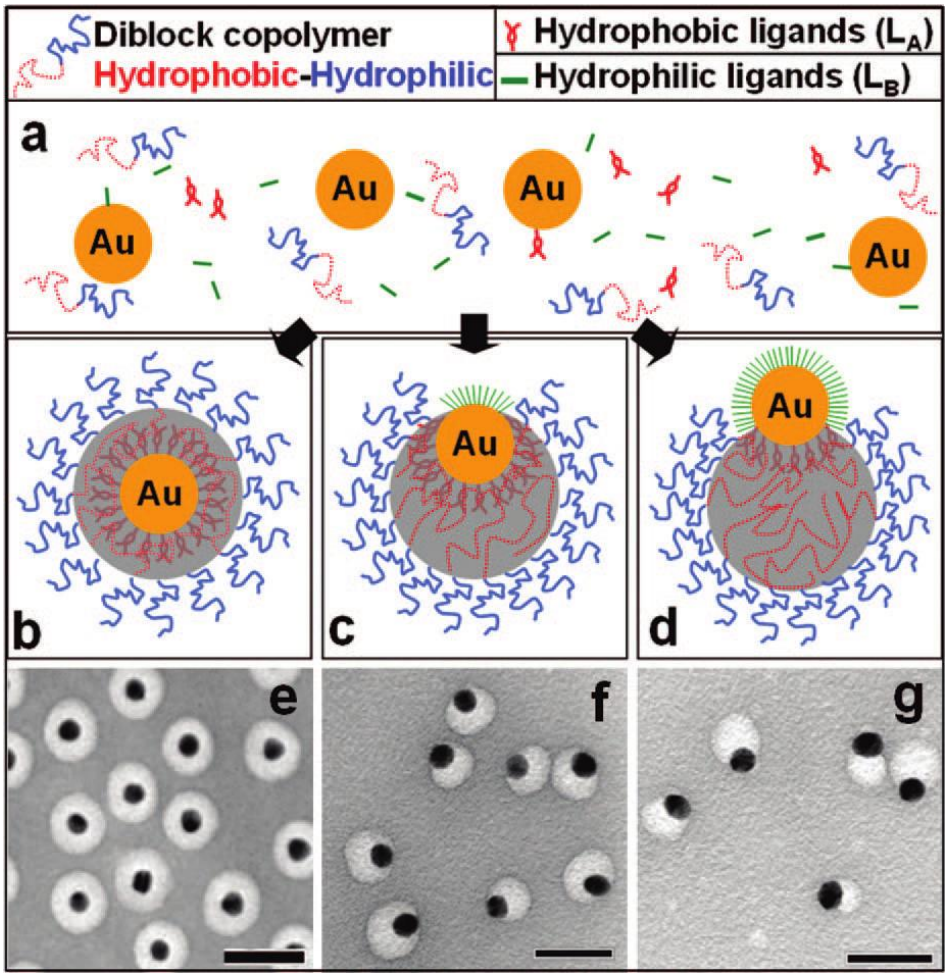

Figure 13. *Synthesis of homocentric and eccentric Au nanoparticles.*
Reproduced with permission from ref 9. Copyright 2008 American Chemical Society

To prepare homocentric gold nanoparticles as shown in Figure 13e, gold nanoparticles were attached to thiolated hydrophobic ligands. This created a full shell that was uniformly surrounded by an amphiphilic copolymer, creating a micelle and a symmetric particle. However, when a hydrophilic ligand was introduced during encapsulation, anisotropic particles were formed as shown in figure 13f and g. This was due to the repulsion between the hydrophilic ligand (green lines figure 13) and the interior of the copolymer. This pushed the hydrophilic ligands to the surface of the particle and installed anisotropy. The shape of the particle could be further tuned by adjusting the ratio of ligands, polymer, and solvent.[9]

Another way to generate anisotropic particles is to use a physical blocker in conjunction with spatially separated ligands.

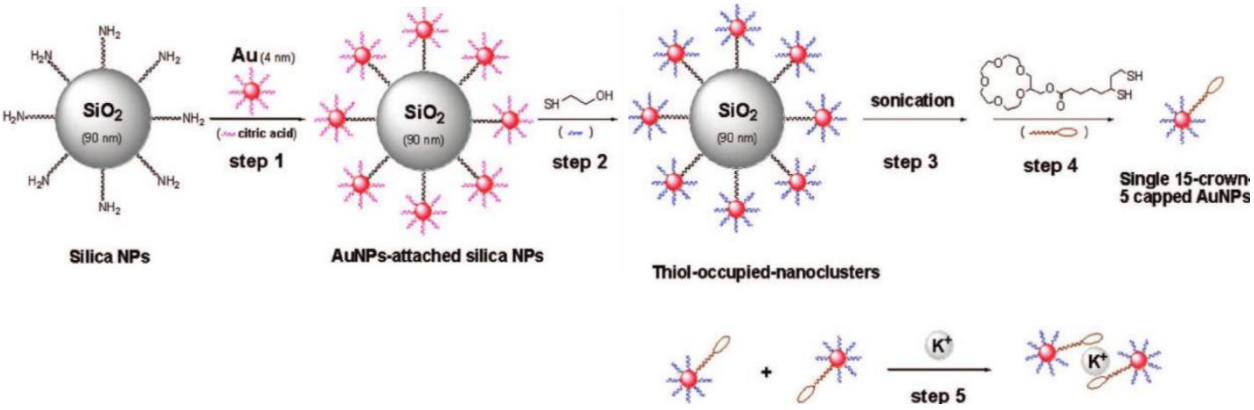

Figure 14. *Scheme for synthesis of single 15-crown-5 functionalized gold nanoparticles.*
Reproduced with permission from ref 9. Copyright 2008 American Chemical Society

Here, gold nanoparticles functionalized with citric acid caps were bound to amine functionalized silica particles due to the stabilization of Au-N bonds. Next, the citric acid cap was exchanged for 2-mercaptoethanol but remained attached to the silica. After sonication, the gold particles were desorbed and had one vacant site. In the presence of 15-crown-5-ether, the vacant site attached to the crown and gave spatially separated functionalized nanoparticles. The particles assembled in the presence of potassium ions through a sandwich interaction of the two crown ethers and potassium ion.[6]

However, without using gold nanoparticles, there is no current way to bring together anisotropic particles with spatially functionalized ligands. To provide chemists with easily accessible, sub-lithographic means of introducing asymmetry on the nanoscale, we are developing a method for anisotropic assembly using nanoparticles covered with different ligands that are spatially separated. By installing functional groups that undergo coupling reactions at the solution-facing end of the ligands, nanoparticles bound with ligands containing complementary coupling partners can be assembled together with spatial selectivity (Figure 15).

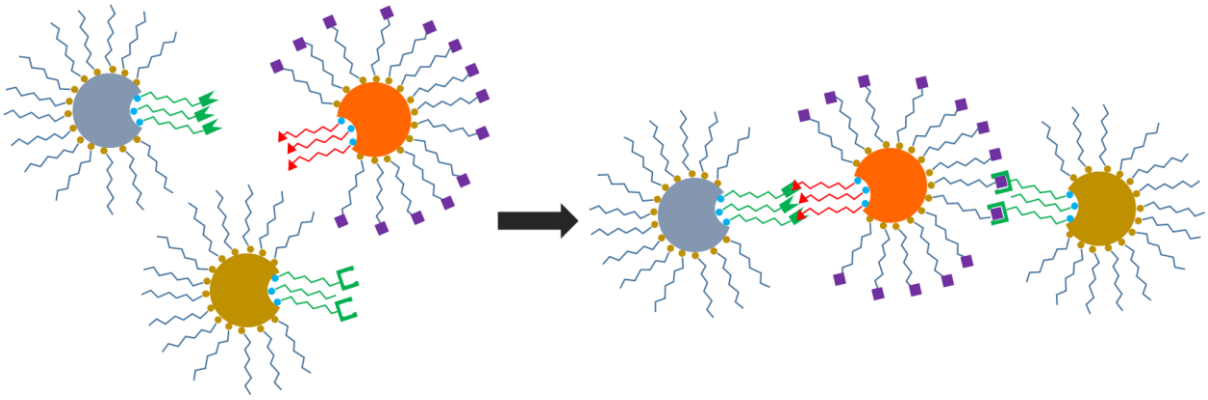

Figure 15. *Directional assembly of spatially functionalized anisotropic particles.*

In order to spatially separate ligands on a nanoparticle, we will be taking advantage of dimer nanoparticles with removable components (Figure 16, below). A strong-binding ligand will first be used to cover the entire dimer particle, followed by selective etching of one component to generate unligated surface on the remaining particle. Subsequent addition of a 2nd ligand terminated with a coupling partner (red triangle) should result in the anisotropic particle needed for spatially selective assembly.

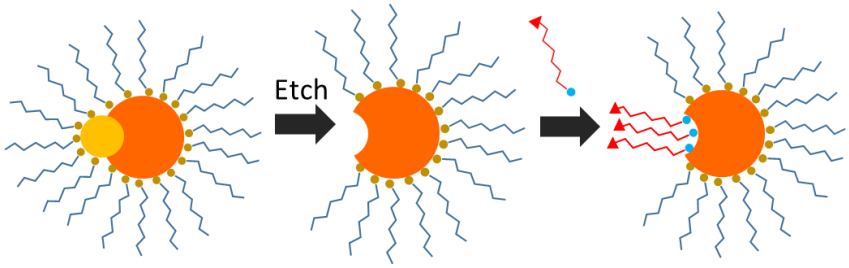

Figure 16. *Generic synthetic scheme for spatially functionalized anisotropic particles*

Specifically, we will be using the well-studied Au-Fe_3O_4 hybrid nanoparticles to generate nanoparticles functionalized with two spatially separated ligands (Figure 17). Starting from an Au-Fe_3O_4 dimer, ligand 1 (shown as the pre-existing purple circles; Figure 17) will be used to cover the surface. Subsequently, the Au domain will be selectively etched away using I_2, resulting in a bowl-shaped Fe_3O_4 particle where the crater exposes unligated Fe_3O_4 surface.[32] A second

ligand (shown as the blue circle; Fig. 17) will then be added and ligate selectively at the exposed crater site, resulting in the desired anisotropic "patchy" Fe_3O_4 nanoparticle. To the best of our knowledge, no anisotropic Fe_3O_4 nanoparticles has been reported in the literature.[10]

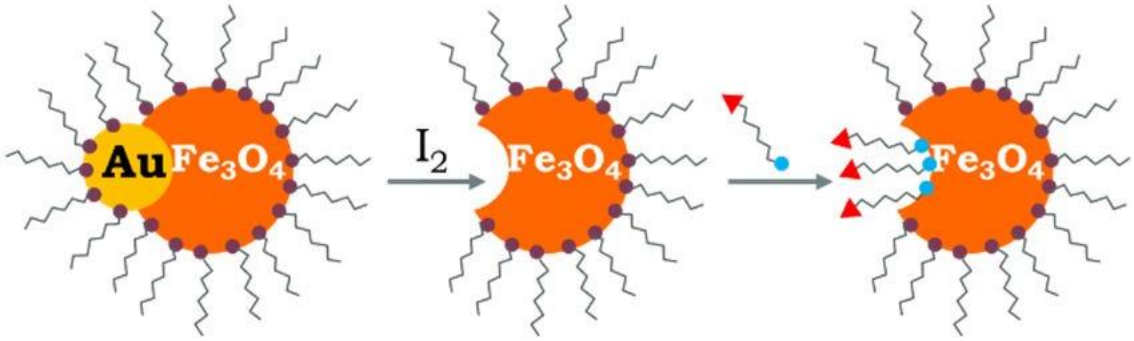

Figure 17. *Synthetic overview of anisotropic Fe_3O_4 nanoparticles with separated ligands.*

Ligand mobility is one nontrivial challenge of our proposed method. To achieve spatial separation of ligands, the first ligand must have very low mobility so migration to the exposed crater site is limited and the crater remains open for preferential binding with the 2nd ligand. However, the binding affinity of the 2nd ligand must also be lower than the 1st ligand so it does not displace the 1st ligand. Therefore, we propose to employ N-heterocyclic carbene (NHC) ligands as the 1st set of ligands, taking advantage of the strong M-C bond between metal sites of the nanoparticle and the carbine ligands.[11] For the 2nd ligand, we propose using diols, which is known to bind the surface of iron oxides tightly but not irreversibly.

To assemble the particles, we have chosen to functionalized the solution facing terminus of the 2nd ligand with either a diene or dienophile, allowing the coupling to take place via the Diels Alder reaction. Additionally, when appropriate partners are chosen the nanoparticle assembly can become reversible by simply changing the reaction temperature.

My work on this project focused on validating whether nanoparticle assembly can take place reversibly using the Diels Alder reaction between furan and maleimide functionalized ligands (Equation 1).

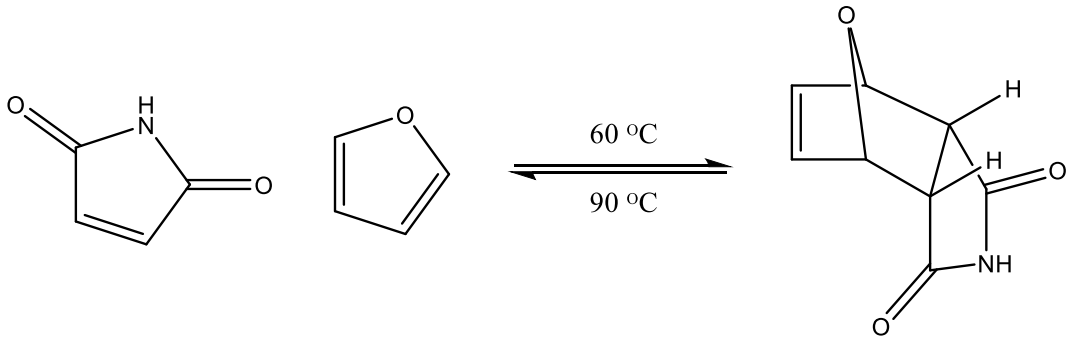

Eqn. 1

Materials and Methods

Gold nanospheres and nanorods: Gold nanosphere (200 nm, 1 OD, supplied in 0.1 mM stabilizing surfactant) was purchased from Strem Chemicals, and gold nanorod (10 nm diam., 1 OD, stabilized by CTAB) was purchased from NanoHybrid Inc.

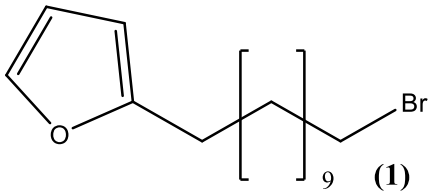

(1)

Dry THF (40 mL) was cooled to -20 °C and *n*-butyl lithium (24 mmol) was added with stirring under argon. Freshly distilled furan (24 mmol) was added dropwise and the mixture was stirred for 4 h. 1,11-dibromoundecane (20 mmol) was added dropwise under vigorous stirring and was brought to room temperature and left overnight. The reaction was quenched with saturated NH_4Cl (20 mL) and washed with ethyl acetate. The product was dried with $MgSO_4$ and evaporated to dryness.

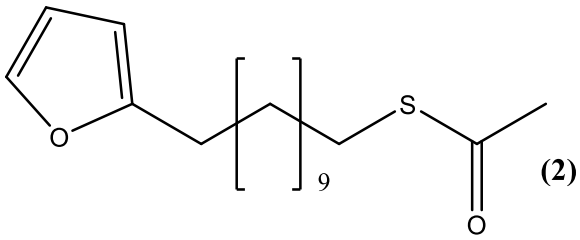

(2)

2-(11-Bromo-undecyl)-furan (1.4 mmol), potassium thioacetate (1.6 mmol) were dissolved in 20 mL acetone and heated at 50 °C overnight. The resulting precipitate was collected and dissolved in 50 mL of dichloromethane, which was washed with water and brine. The mixture was then dried with $MgSO_4$ and evaporated to dryness, affording a pale yellow oil.

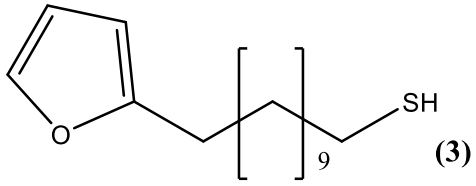

(3)

Thiolate **2** was dissolved in 10 mL of argon purged methanol. 1M NaOH in ethanol was added and stirred at room temperature for 50 minutes. The solvent was removed and the residue was dissolved in dichloromethane, washed with water and brine, and dried with Mg_2SO_4. The organic mixture was evaporated to dryness affording a pale yellow oil.

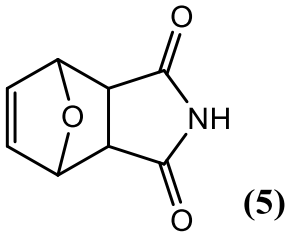

(5)

Maleimide (1.0g, 10.3 mmol) and furan (1.05 g, 15.5 mmol) were dissolved in 15 mL of diethyl ether in a sealed tube and was heated at 95 °C overnight. The Diels Alder product precipitated after cooling and was washed with cold diethyl ether, removing the unreacted maleimide. This produced **5**, a white crystalline powder.

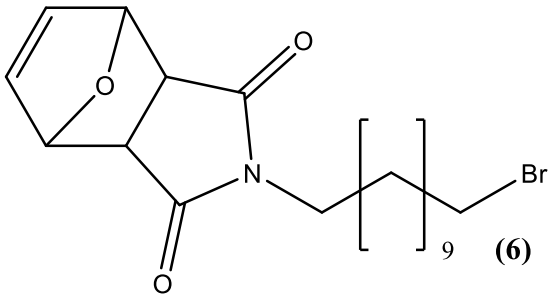

(6)

1,11-dibromoundecane (11.6 mmol), compound **5** (5.8 mmol), and K_2CO_3 (5.8 mmol) were dissolved in 25 mL dimethylformamide and heated to 50 °C overnight. The residue was dissolved in dichloromethane, washed with water, dried with Mg_2SO_4, and rotary evaporated to dryness.

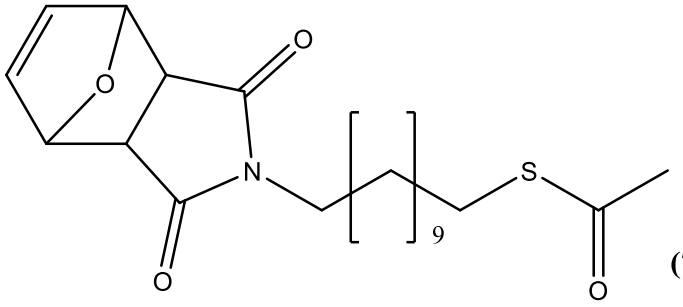

(7)

Compound **6** (1.4 mmol), potassium thioacetate (1.6 mmol), were dissolved in 20 mL of acetone and heated at 50 °C overnight. The resulting precipitate was collected and dissolved in 50 mL of dichloromethane, which was washed with water and brine. The mixture was then dried with $MgSO_4$ and evaporated to dryness, affording a pale yellow oil.

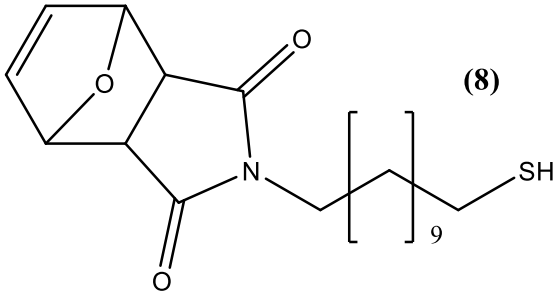

(8)

Thiolate **7** was dissolved in 10 mL of argon purged methanol. 1M NaOH in ethanol was added and stirred at room temperature for 50 minutes. The solvent was removed and the residue

was dissolved in dichloromethane, washed with water and brine, and dried with Mg_2SO_4. The organic mixture was evaporated to dryness affording a pale yellow oil.

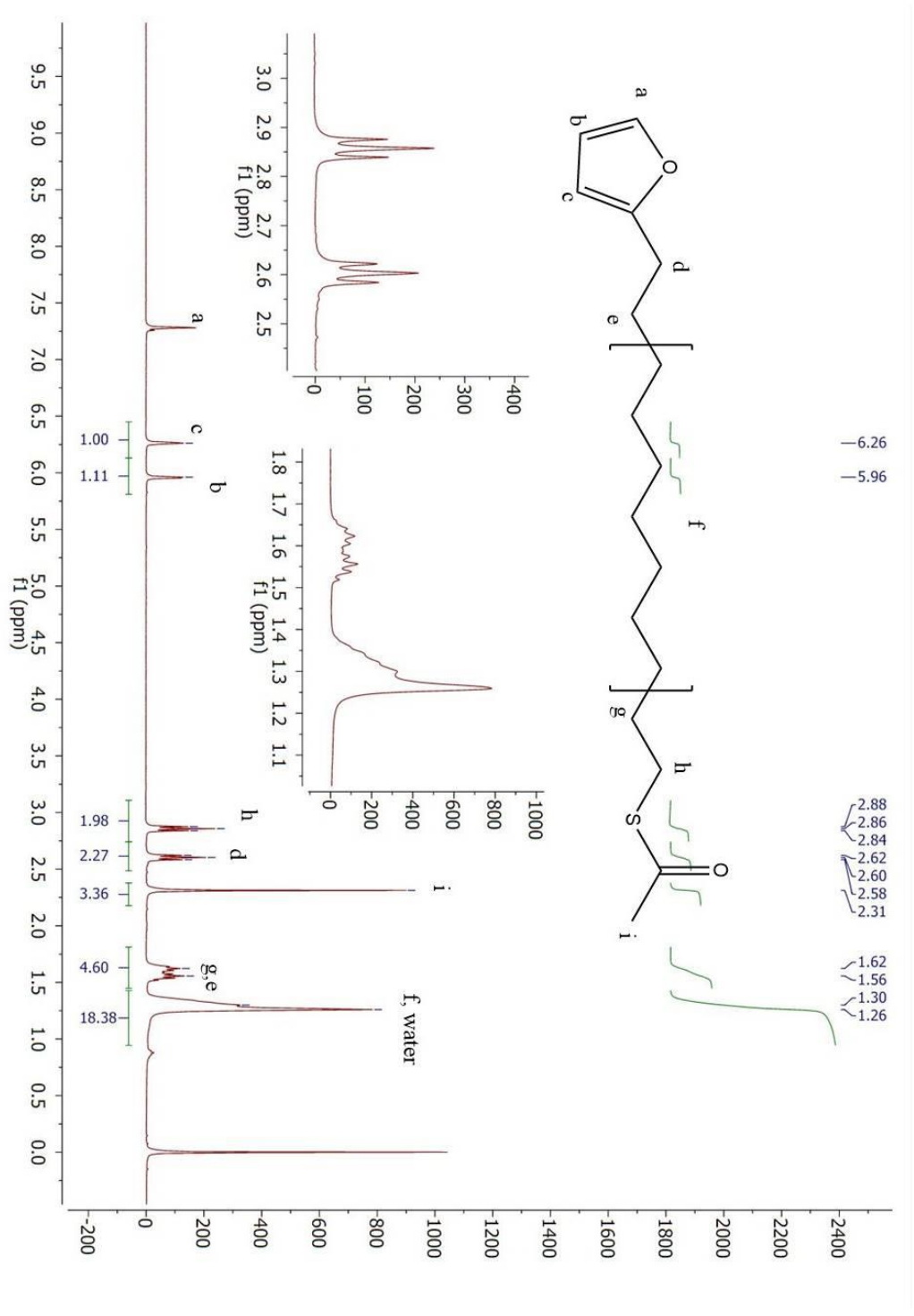

Figure 18. *NMR of thiolated furan.*

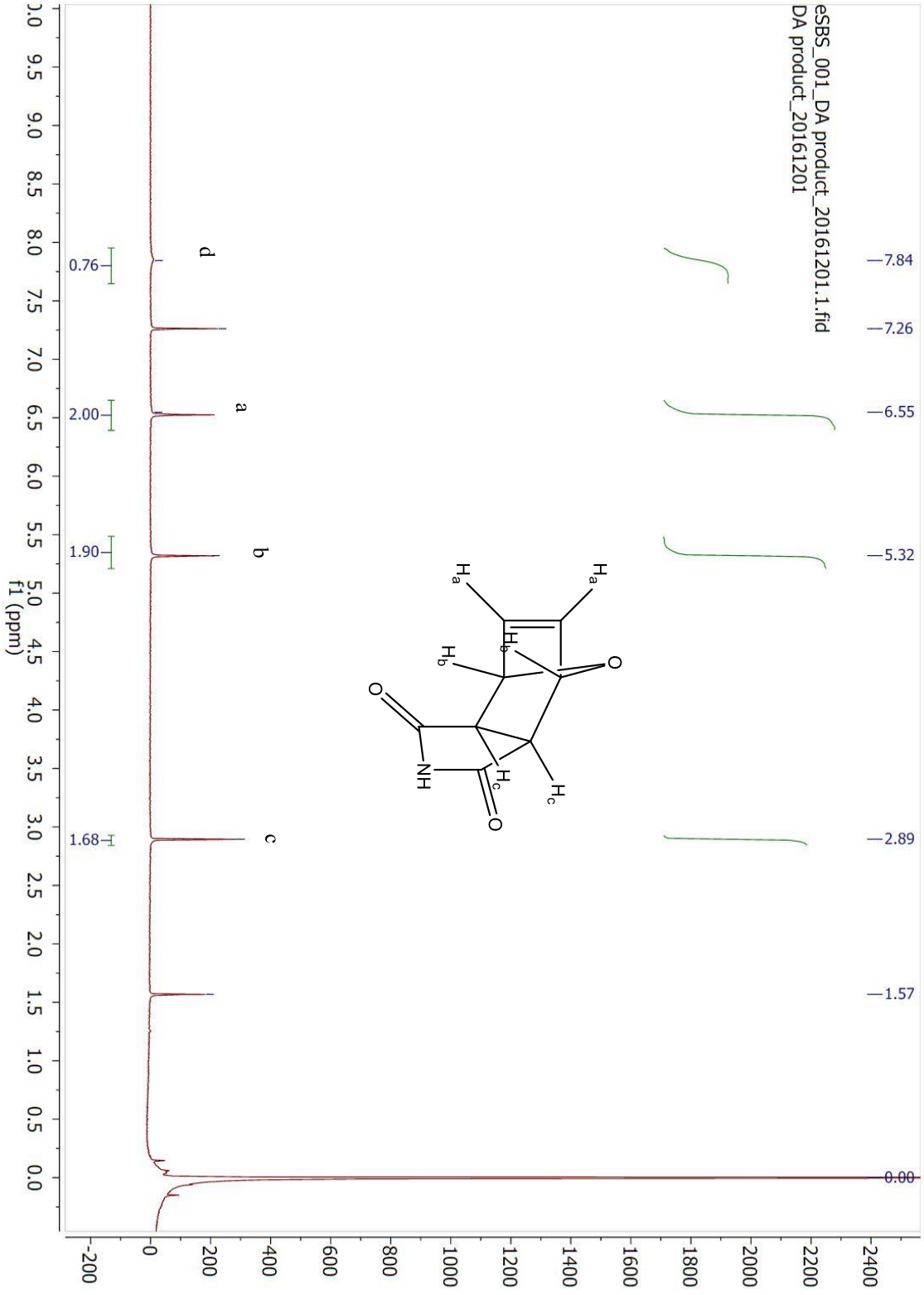

Figure 19. *NMR of maleimide and furan Diels Alder product.*

Results and Discussions

To avoid complication from the challenge of ligand mobility I have chosen to test assembly on gold nanoparticles of different morphology. Specifically, thiol ligands were used to bind to gold nanospheres and nanorods. For the nanospheres (200 nm diameter), thiol ligand functionalized with the furan moiety was used and for the nanorods (10 nm diameter x 40 nm length), the thiol ligand was functionalized with maleimide. Ligands with eleven-carbon alkyl chain were chosen as this chain length should be sufficiently long to connect two gold nanoparticles without introducing any steric repulsion

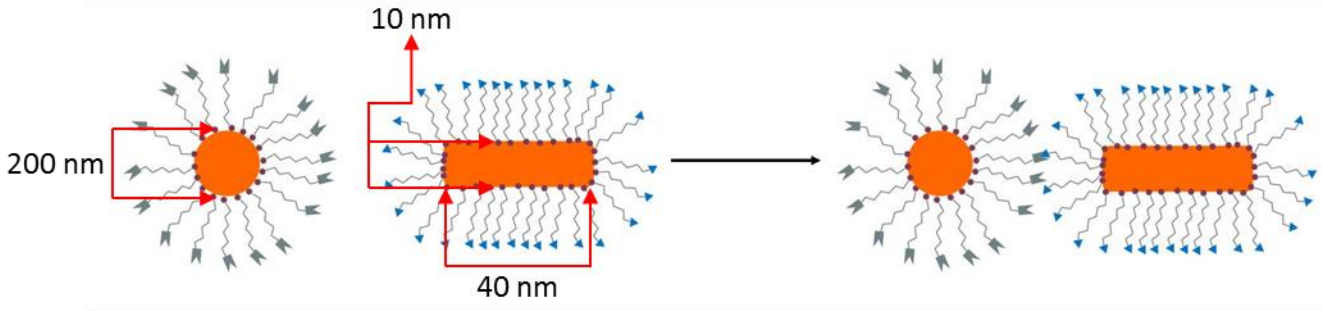

Figure 20. *Reversible assembly of gold nanospheres and nanorods.*

To synthesize the ligands (figures 21 and 22), n-butyl lithium was used to deprotonate furan and maleimide. Subsequently, 1,11-dibromoundecane was added and undergoes an S_N2 reaction with furan/maleimide to generate compounds (1) and (6). Next, thioacetate underwent a second S_N2 with the terminal bromine to generate compounds (2) and (7). The resulting thioester

underwent hydrolysis to form thiols (3) and (8), which could then be deprotonated in the presence of gold nanoparticles to create the final ligated particles.

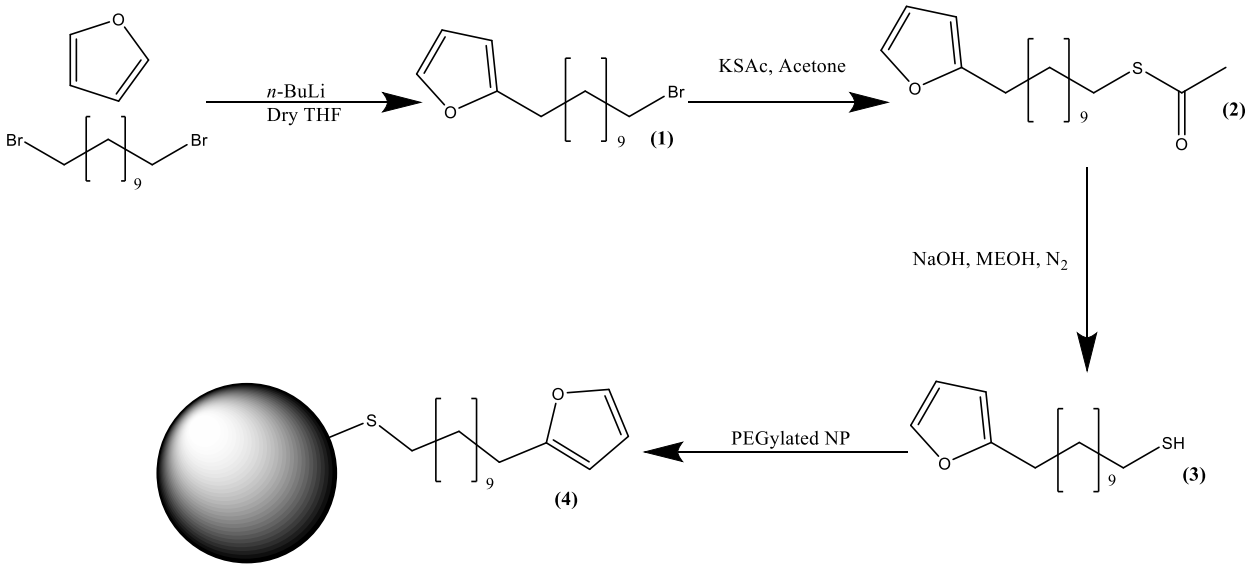

Figure 21. *Synthetic scheme for the furan tether.*

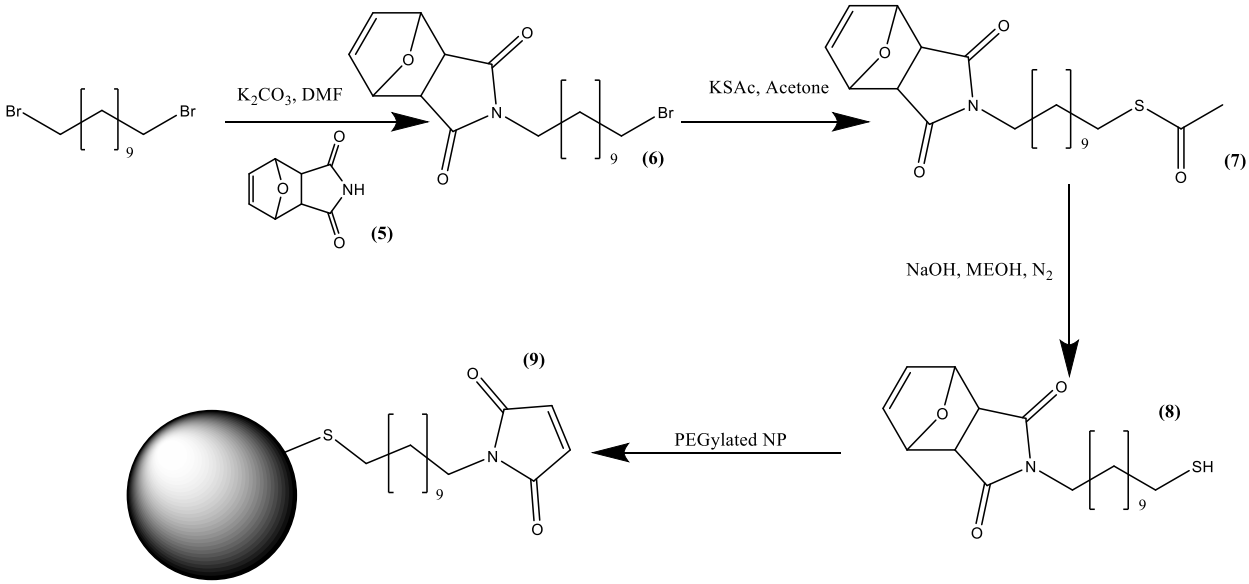

Figure 22. *Synthetic scheme for the maleimide tether.*

Compound 2 was synthesized cleanly and only needs to be converted to the thiol before attachment to the gold nanoparticles. The protected maleimide was made and used in the synthesis of compound 6. Currently, compound 6 is being purified before conversion to the

thioacetate. The synthesis of the two ligands provided groundwork for the overall project. In the future, the ligands will be added to gold nanoparticles and then reacted under Diels Alder conditions to test assembly. Once assembly is confirmed with the gold system, work can be done on synthesizing the corresponding ligands with NHC functionality for binding to Fe_3O_4 nanoparticles.

References

1. Wu, X.-L., Jiang, L.-Y., Cao, F.-F., Guo, Y.-G. & Wan, L.-J. LiFePO $_4$ Nanoparticles Embedded in a Nanoporous Carbon Matrix: Superior Cathode Material for Electrochemical Energy-Storage Devices. *Adv. Mater.* **21,** 2710–2714 (2009).
2. Muller, R. H. & Keck, C. M. Challenges and solutions for the delivery of biotech drugs – a review of drug nanocrystal technology and lipid nanoparticles. *J. Biotechnol.* **113,** 151–170 (2004).
3. Liu, H. *et al.* A review of anode catalysis in the direct methanol fuel cell. *J. Power Sources* **155,** 95–110 (2006).
4. Navarro, R. M., Alvarez-Galván, M. C., Villoria de la Mano, J. a., Al-Zahrani, S. M. & Fierro, J. L. G. A framework for visible-light water splitting. *Energy Environ. Sci.* **3,** 1865 (2010).
5. Hodges, J. M., Morse, J. R., Williams, M. E. & Schaak, R. E. Microscopic Investigation of Chemoselectivity in Ag–Pt–Fe_3O_4 Heterotrimer Formation: Mechanistic Insights and Implications for Controlling High-Order Hybrid Nanoparticle Morphology. *J. Am. Chem. Soc.* **137,** 15493–15500 (2015).
6. Ho, M. L. *et al.* 15-Crown-5 functionalized au nanoparticles synthesized via single molecule exchange on silica nanoparticles: its application to probe 15-crown-5/k +/15-crown-5 ‘sandwiches’ aslinking mechanisms. © 2009 American Chemical Society. *J. Phys. Chem. C* **113,** 1686–1693 (2009).
7. Mirkin, C. A., Letsinger, R. L., Mucic, R. C. & Storhoff, J. J. A DNA-based method for rationally assembling nanoparticles into macroscopic materials. *Nature* **382,** 607–609 (1996).
8. Miyanohata, R., Matsushita, T., Tsuruoka, T., Nawafune, H. & Akamatsu, K. A facile template synthesis of asymmetric gold silica heteronanoparticles. *J. Colloid Interface Sci.* **416,** 147–150 (2014).
9. Chen, T., Yang, M., Wang, X., Huey Tan, L. & Chen, H. Controlled Assembly of Eccentrically Encapsulated Gold Nanoparticles. doi:10.1021/ja8040288
10. Lee, Y., Garcia, M. A., Frey Huls, N. A. & Sun, S. Synthetic Tuning of the Catalytic Properties of Au-Fe3O4 Nanoparticles. *Angew. Chemie Int. Ed.* **49,** 1271–1274 (2010).
11. Crudden, C. M. *et al.* Ultra stable self-assembled monolayers of N-heterocyclic carbenes on gold. *Nat. Chem.* **6,** 409–14 (2014).

Academic Vita

Sarah Bevilacqua
sarahbev13@gmail.com

OBJECTIVE: To enter a Ph. D. program in heterogeneous material catalysis

EDUCATION

The Pennsylvania State University, University Park, PA
BS, Chemistry; Minor, Statistics; Honors in Chemistry — Anticipated May 2017
Institut Américain Universitaire, Aix-en-Provence, France — May 2014 – Aug 2014

HIGHLIGHTS

- Skilled in both colloidal material and organic synthesis and characterization
- Proficient in R, Python, SAS, and JMP.
- Experience in cell culture, mouse handling, and molecular biology techniques such as RT-qPCR and western blots.

RESEARCH EXPERIENCE

Prof. Raymond Schaak – Heterogeneous Materials as Catalysts **(2016 – Present)**
- Synthesized mixed metal materials using colloidal synthesis and characterized structures using XRD and TEM
- Tested materials as catalysts for the Sonogashira coupling reaction and analyzed products with NMR and GC

Unilever R&D – Product Development for Dove Core Body Wash **(May 2016 – Aug 2016)**
- Mathematically modeled lather characteristics of different surfactant formulations using JMP
- Created dissipative particle dynamics (DPD) model of surfactants in parallel with Port Sunlight Laboratory

Prof. Michael Green – Determining the Redox Potential of Compound I in CYP 158A2 **(Dec 2014 – Nov 2015)**
- Grew and characterized cytochrome P450 variants using stopped-flow UV-Vis, freeze-quench, Mössbauer spectroscopy, and EXAFS
  - Synthesized ^{57}Fe-heme to modify and characterize horseradish peroxidase

Dean Douglas Cavener – Elucidating the Role of PERK EIF2AK3 in Proinsulin Processing **(Aug 2013 – Nov 2014)**
- Worked to understand the role of protein SDF2L1 and EIF2AK3 in the PERK signaling pathway in mice through gene expression techniques

PUBLICATIONS

- "PERK EIF2AK3 regulates proinsulin processing by controlling ER chaperones and not by regulating protein synthesis." Carrie R. Lewis, Rong Wang, Jingjie Hu, **Sarah Bevilacqua**, Rebecca A. Bourne, Barbara C. McGrath, James C. Paton, Adrienne W. Paton, Sophie Collardeau-Frachon, and Douglas R. Cavener. *(submitted)*

SELECTED POSTER PRESENTATIONS

- **Sarah Bevilacqua**, Nathanial Long, Eric Piechota, Bratoljub Milosavljevic "*Charge Effect of Adsorption onto Colloidal Silica Surfaces: An in situ Laser Photolysis Study*." National ACS Conference, March 2016, San Diego, CA
- **Sarah Bevilacqua,** Timothy Yosca, Michael Green *"Determination of the Reduction Potential of Compound I in Cytochrome P450 158A2"* Central PA Section of the ACS, September 2015, State College, PA

TEACHING EXPERIENCE

2016 – Present Teaching Assistant for Organic Chemistry Mechanisms, The Pennsylvania State University
2016 – Present Teaching Assistant for Organic Chemistry Lab, The Pennsylvania State University

CLUBS AND ACTIVITIES

Springfield Benefiting the Penn State Dance Marathon: Executive board – Donor & Alumni Relations **(2013 – Present)**
- Leads a club that raises over $270,000/year for pediatric cancer patients and research
- Communicates between alumni, donors, and general members orally and through emails and social media

Science LionPride: Chair – Webmaster **(2013 – Present)**
- Represents Eberly College of Science to alumni, current students, prospective students, and community
- Created and maintains professional website for club

AWARDS/HONORS

2016 Tea's Scholarship
2015 3M Grant recipient
2014 President Sparks Award
2013 President's Freshman Award
2013 – Present Schreyer Honors Academic Excellence Award
2013 – Present Dean's List